



Pergamon

Acta mater. 48 (2000) 4571–4576



www.elsevier.com/locate/actamat

## MULTIPLE SCATTERING FROM RUTILE TiO<sub>2</sub> PARTICLES

L. E. MCNEIL\*‡ and R. H. FRENCH

DuPont Central Research and Development, Wilmington, DE 19880-0356, USA

**Abstract**—The physical properties of rutile titania (TiO<sub>2</sub>) have led to its wide use as a white pigment in many applications. The success of these applications depends not only on the optical properties of the bulk material, but also on subtle aspects of the scattering of light from collections of small TiO<sub>2</sub> particles embedded in a transparent medium. We consider here the problem of multiple scattering in dense systems containing particles of a size comparable to the wavelength. Our method of analysis allowed us to understand the effects that the number density of particles and the particle size distribution have on the measured diffuse reflectance of such films. We apply this analysis to films of TiO<sub>2</sub> particles in a transparent medium. We present the results of diffuse reflectance and transmittance measurements in the visible range of films with concentrations that span the range in which the radiation fields of adjacent particles begin to interact. We find that for  $\lambda < 400$  nm the spectra are predominantly determined by the scattering properties of the individual single particles. At longer wavelengths, where multiple-scattering effects become important, the particles behave as independent scatterers for volume concentrations of less than approximately 1%. At higher concentrations, where the interparticle spacing becomes less than the wavelength of light in the medium, the interaction of the radiation fields of adjacent particles lowers the backscattering fraction of the multiple-scattering function. This reduction in backscattering is significant for many of the applications of films containing TiO<sub>2</sub>, such as coatings and paper, which rely upon multiple scattering from large numbers of particles to provide the desired opacity. © 2000 Acta Metallurgica Inc. Published by Elsevier Science Ltd. All rights reserved.

*Keywords:* Optical properties; Reflectivity; Absorption & transmission

### 1. INTRODUCTION

The physical properties of rutile titania (TiO<sub>2</sub>), including its transparency at visible wavelengths and its large index of refraction, have made it the world's most widely used white pigment for coatings, plastics and paper [1]. The success of these applications depends not only on the optical properties of the bulk material, but also on subtle aspects of the scattering of light from collections of small TiO<sub>2</sub> particles embedded in a transparent medium. The problem of scattering of electromagnetic radiation from a single small particle was solved long ago, and exhaustive treatments exist in the literature [2, 3]. The problem of multiple scattering, in which the light scattered from one particle impinges upon another, has also been addressed by many authors [4–11] in different regimes of particle size, number density and absorp-

tion. We have developed a method of analysis that allows us to understand the effects that the number density of particles and the particle size distribution have on the measured diffuse reflectance of such films. We apply this analysis to films of TiO<sub>2</sub> in a transparent medium. We take as our starting point the Kubelka–Munk two-stream model [13–17], which is valued for its simplicity, if not for its fidelity to the actual experimental situation. TiO<sub>2</sub> particles are non-absorbing except at very short wavelengths, and their large index of refraction leads to very strong scattering. Furthermore, the particles considered here are of a size to give maximum scattering per unit volume of particle in the middle of the visible range; i.e., they are optimally sized. This maximal scattering causes each particle to extend its influence into a large volume, so that even at low number density the radiation fields of adjacent particles may not be independent of one another. This system therefore provides a test of the utility of our method of analysis.

We present here the results of measurements of diffuse reflectance and transmittance in the visible range of films consisting of 200 nm TiO<sub>2</sub> particles in a resin matrix. The number density of particles in the films is such that the particles occupy 1–3% of the total

\* To whom all correspondence should be addressed. Tel.: 001 919 962 7204; fax: 001 919 962 0480.

E-mail address: mcneil@physics.unc.edu (L.E. McNeil)

‡ Permanent address: Department of Physics and Astronomy, University of North Carolina at Chapel Hill, Chapel Hill, NC 27599-3255, USA.

volume of the films. Calculations [18–20] of the near-field distribution of the scattered intensity have shown that at such concentrations the particles approach one another closely enough that their radiation fields begin to interact. This interaction modifies the calculated scattering coefficient of the assembled particles, and is therefore expected to modify the measured diffuse reflectance. The results presented here confirm this expectation.

In our analysis of these results, we make use of a model of multiple scattering we have developed, which is presented in detail elsewhere with application to resonant, strongly absorbing, red pigment particles [12]. This model connects the experimentally straightforward measurements of diffuse reflectance and transmission of the film with the fundamental optical properties and scattering characteristics of the materials of which the film is made, by making use of the simple Kubelka–Munk formulation. The computational simplicity of this formulation has allowed its practitioners to develop a large base of empirical knowledge, but it has thus far been difficult to connect that knowledge base with an understanding of the fundamental optical properties of the materials. Our model allows such a connection to be made, and thus makes it possible to analyze the effects that modifications in the particulate microstructure, such as particle size, number density, absorption, agglomeration and other characteristics, will have on the measured diffuse reflectance and transmission spectra.

## 2. EXPERIMENT

### 2.1. Sample preparation and measurements

The TiO<sub>2</sub>–resin samples were prepared by D. E. Spahr of DuPont Automotive Products (Philadelphia, PA). Appropriate quantities of R-960 TiO<sub>2</sub> (diameter  $a = 200$  nm) were suspended in an acrylic resin, the resulting slurry was ground in a media mill to break up agglomerates, and the films were drawn by hand using a 1.5 mil (38.1  $\mu\text{m}$ ) blade. The substrates were 0.090 in. thick, Viosil fused quartz plates from DuPont Photomask, manufactured by Shin-Etsu Chemical Co. The films were baked at 250°F (121°C) for 30 min to evaporate the solvent. The final thicknesses of the films were 12.6–15.4  $\mu\text{m}$ , measured with a Dektak IIA surface profilometer to an accuracy of  $\pm 1$   $\mu\text{m}$ . The particle volume concentrations (PVCs) were 1.05%, 1.6% and 3%. The total transmission (direct + diffuse) at 550 nm was in the range 42–63%.

Measurements of total and diffuse reflectance and transmittance of the films were made by using a Lab-sphere model RSA-PE-19 reflectance spectroscopy accessory (integrating sphere) attached to a Perkin–Elmer Lambda 19 UV/VIS/NIR spectrophotometer. The instrument is a dual-beam one, and uses a halogen lamp for illumination at wavelengths longer than 319 nm and a deuterium lamp at shorter wave-

lengths. Data were acquired over the wavelength range 250–850 nm, and were referenced to a normalized background. The scan rate was 60 nm/min, and data were taken at 1 nm intervals. The nominal band pass was 2 nm, corresponding to an actual spectral bandwidth ranging from 2.02 nm at short wavelengths to 1.69 nm at long wavelengths. For transmittance measurements the light was normally incident on the back side of the quartz substrate, so that it passed through the substrate before encountering the film, and a quartz blank without film was placed in the reference beam. For reflectance measurements the light was incident directly on the film at an angle of 8° to the film normal. All measurements were made under ambient conditions.

For measurements of diffuse reflectance and transmittance, the specularly reflected or directly transmitted light was removed from the signal by placing a light trap at the appropriate position on the integrating sphere. The trap removed the light from a cone of half-angle  $\sim 4.2^\circ$  around the directly transmitted beam from the transmittance measurements, and  $\sim 7.0^\circ$  around the specularly reflected beam from the reflectance measurements.

### 2.2. Single-scattering calculations

The scattering and absorption cross-sections  $C_{\text{sca}}$  and  $C_{\text{abs}}$  for a single 200 nm diameter TiO<sub>2</sub> sphere embedded in acrylic resin were calculated in the Mie theory using the BHMIE computer code by Bohren and Huffman [2]. From these we obtained the volume-normalized scattering and absorption coefficients  $S = C_{\text{sca}}/(\pi a^3/6)$  and  $K = C_{\text{abs}}/(\pi a^3/6)$ . Calculations were carried out for wavelengths in the range 250–850 nm at 10 nm intervals using the appropriate values for the optical constants of the particle and the medium. TiO<sub>2</sub> is birefringent, with a different index of refraction for light polarized perpendicular or parallel to the optic axis, so the “average index” approximation [18–20] was used. In this approximation the TiO<sub>2</sub> particle is assumed to be isotropic, with real and imaginary parts of the refractive index equal to  $n_{\text{particle}} = (2n_o + n_e)/3$  and  $k_{\text{particle}} = (2k_o + k_e)/3$ , where  $n_o$  and  $k_o$  ( $n_e$  and  $k_e$ ) are the ordinary (extraordinary) index of refraction and extinction coefficient. The values for the optical constants were taken from the literature [21], with linear interpolation applied at wavelengths for which values were not available. The optical constants as a function of wavelength for the resin in which the particles are embedded were taken from ellipsometric measurements of the resin (without particles) by M. F. Lemon of DuPont. The real index  $n_{\text{medium}}$  of this resin ranges from 1.5959 at  $\lambda = 250$  nm to 1.4448 at  $\lambda = 850$  nm, and its extinction coefficient  $k_{\text{medium}} < 0.004$  at all wavelengths. The relative refractive index (index contrast)  $m = n_{\text{particle}}/n_{\text{medium}}$  ranges from approximately 1.3 to 1.8 over this wavelength range. The Mie size parameter  $x = 2\pi a n_{\text{medium}}/\lambda$ , where  $a$  is the diameter of the sphere, ranges from 19.9 to 5.4. The particles are

therefore not small compared with the wavelength (in which case Rayleigh theory would apply), nor are they large enough to be in the regime of geometrical optics. In order to examine the angular distribution of the scattering, calculations of the angular distribution function

$$G(\cos \theta) = \frac{1}{k^2 C_{\text{sca}}} \frac{dC_{\text{sca}}}{d\Omega}$$

(where  $k$  is the wavenumber  $k = 2\pi/\lambda$ , with  $\lambda$  the wavelength of light in the medium) were also made using the MIETAB program.\*

### 2.3. Data analysis

In analyzing the reflection and transmission data, we followed a method derived from the Kubelka–Munk two-stream model of multiple scattering. In the Kubelka–Munk model [13–15] of diffuse reflectance and transmission from a slab, the scattered light consists of two streams, one of which is forward-directed (perpendicular to the slab and in the direction of incidence) and the other of which is backward-directed (opposite to the direction of incidence). The slab is assumed to consist of a homogeneous material (rather than the more realistic case of particles in a medium) characterized by absorption parameter  $K^*$  and scattering parameter  $S^*$ . These parameters are not assumed to have any particular relation to the optical constants of the material of which the slab is made. The solution of the resulting differential equations for the forward and backward streams results in expressions for the diffuse reflectance  $R$  and diffuse transmission  $T$  as functions of  $K^*$ ,  $S^*$  and the slab thickness  $d$ :

$$R = \frac{(1 - \beta^2) \sinh \kappa d}{(1 + \beta^2) \sinh \kappa d + 2\beta \cosh \kappa d} \quad (1)$$

and

$$T = \frac{2\beta}{(1 + \beta^2) \sinh \kappa d + 2\beta \cosh \kappa d} \quad (2)$$

where

$$\beta = \sqrt{\frac{K^*}{K^* + 2S^*}}$$

and

$$\kappa = \sqrt{K^*(K^* + 2S^*)}.$$

Given experimentally measured values of  $R$  and  $T$  at various wavelengths for a film of known thickness, the Kubelka–Munk parameters  $K^*$  and  $S^*$  as functions of  $\lambda$  can be extracted by fitting equations (1) and (2) to the experimental data, with  $K^*$  and  $S^*$  as fitting parameters. We performed these fits using the GRAMS/32 software from Galactic Industries Corp., with additional computer code provided by Deconvolution and Entropy Consulting.† In essence the Kubelka–Munk model is serving as a parametrization of the reflectance and transmittance data.

In order to relate the Kubelka–Munk scattering parameter  $S^*$  to the single-particle scattering coefficient  $S$ , we follow a method suggested by Mudgett and Richards [11] and develop it more fully. Mudgett and Richards noted that the diffuse scattering (and thus  $S^*$ ) could be thought of as resulting from a convolution of two factors: single-particle scattering, which redirects the incident light according to the angular distribution given by  $G(\cos \theta)$ ; and multiple scattering, in which the light scattered from one particle is incident upon a subsequent particle from a direction other than that at which it was incident upon the first. The strength of the scattering from each particle is described by the single-particle scattering coefficient  $S$  obtained from Mie theory. The Kubelka–Munk scattering parameter thus becomes

$$S^* = S \int_{-1}^1 F(\cos \theta) G(\cos \theta) d(\cos \theta), \quad (3)$$

where  $F(\cos \theta)$  contains the multiple-scattering information. The function  $F$  incorporates the microstructure of the arrangement of particles in the film, and can be expected to change with particle number density, agglomeration of the particles into clusters, and film thickness. This convolution can be simplified by expanding both  $G$  and  $F$  in Legendre polynomials:

$$G(\cos \theta) = \sum_{n=0}^{\infty} a_n P_n(\cos \theta) \quad \text{and} \quad (4)$$

† GRAMS is available from Galactic Industries, 325 Main Street, Salem, NH 03079, USA (<http://www.galactic.com>). The programs used here are available as part of Electronic Structure Tools from Deconvolution and Entropy Consulting, 755 Snyder Hill Road, Ithaca, NY 14850, USA; tel.: +1-607-272-0645; E-mail: [lin.denoyer@deconvolution.com](mailto:lin.denoyer@deconvolution.com) (<http://www.deconvolution.com>).

\* The MIETAB program was obtained from A. Miller ([amiller@nmsu.edu](mailto:amiller@nmsu.edu)).

$$F(\cos \theta) = \sum_{m=0}^{\infty} b_m P_m(\cos \theta).$$

For a spherical particle, it is straightforward to calculate the coefficients  $a_n$  of the expansion of the single-particle function  $G$ . For convenience, we have chosen to obtain the coefficients by fitting the function  $G$  obtained using the MIETAB program to a polynomial of the form found in equation (4), using the  $a_n$  as fitting parameters. For particles that are comparable in size to the wavelength of the light, the sharply peaked character of  $G$  requires as many as 22 terms to obtain a good approximation with a finite expansion. The integral in equation (3) then reduces to

$$S^* = S \sum_l \frac{2a_l b_l}{2l + 1}. \quad (5)$$

By fitting equation (5) to the measured values of  $S^*$ , using  $S$  derived from Mie theory, the coefficients  $b_l$ , and thus the function  $F(\cos \theta)$ , can be extracted. Both  $S^*$  and  $S$  vary with wavelength, but since for any single wavelength equation (5) can be satisfied with an infinite number of sets of  $b_l$ , it is necessary to restrict the values of the  $b_l$  to be the same at all wavelengths. (This limitation is typical of those required in solving an "inverse problem".) As for the extraction of  $K^*$  and  $S^*$ , we have performed this fit using the GRAMS/32 software from Galactic Industries Corp., together with the programs K-MUNK, GFIT and GFIT-S provided by Deconvolution and Entropy Consulting.

### 3. RESULTS AND DISCUSSION

The single-particle scattering and absorption coefficients  $S$  and  $K$  for a 200 nm diameter TiO<sub>2</sub> sphere calculated from Mie theory are shown in Fig. 1. The

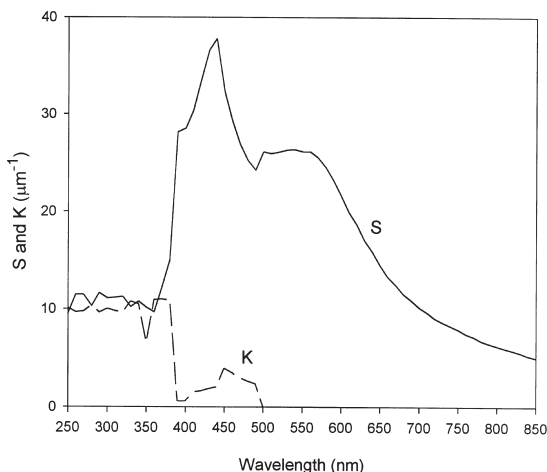


Fig. 1. Scattering coefficient  $S$  (solid line) and absorption coefficient  $K$  (broken line) for a single 200 nm TiO<sub>2</sub> sphere as a function of wavelength, calculated from Mie theory.

extinction coefficient  $k_{\text{particle}}$  of TiO<sub>2</sub> is negligible for wavelengths  $\lambda > 500$  nm, and so  $K = 0$  in that range. The scattering coefficient increases sharply near  $\lambda = 400$  nm, has a maximum near 450 nm, and declines more slowly at higher wavelengths. These characteristics are controlled primarily by the variation in the index of refraction of TiO<sub>2</sub> with wavelength.

The diffuse reflectance spectra for films of three different PVCs are shown in Fig. 2, normalized to their maximum value. The actual maximum reflectance is  $R = 0.20$  for the 1.05% film, 0.31 for the 1.6% film, and 0.46 for the 3% film. Also shown is the single-particle or "Mie reflectance"  $R_M$ , similarly normalized.  $R_M$  embodies the characteristics of the reflectance spectrum that result from scattering from a single particle. It is calculated by integrating the angular distribution function  $G$  over the backward hemisphere ( $-1 < \cos \theta < 0$ ), and dividing by the integral over the full sphere. This is then multiplied by the scattering efficiency  $C_{\text{sca}}/\pi(a/2)^2$ , and by the albedo  $C_{\text{sca}}/(C_{\text{sca}} + C_{\text{abs}})$ . (For  $\lambda > 500$  nm, where  $C_{\text{abs}} = 0$ , the albedo is equal to unity.) Thus

$$R_M = \frac{\int_{-1}^0 G(\cos \theta) d(\cos \theta)}{\int_{-1}^1 G(\cos \theta) d(\cos \theta)} \frac{C_{\text{sca}}}{\pi(a/2)^2} \frac{C_{\text{sca}}}{C_{\text{ext}}}. \quad (6)$$

The comparison of  $R_M$  with the measured reflectance in Fig. 2 shows that the features appearing in the spectrum at wavelengths below 400 nm result from the single-particle scattering. The effects due to multiple scattering appear at higher wavelengths.

The Kubelka-Munk scattering parameter  $S^*$  curve for these films has a shape versus wavelength very similar to that of the diffuse reflectance itself. The

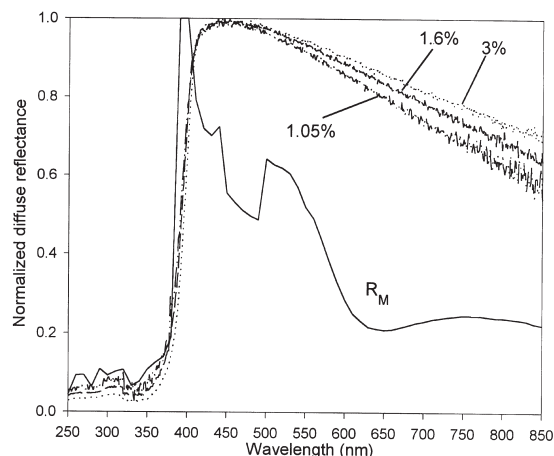


Fig. 2. Normalized values of diffuse reflectance for films with particle volume concentrations as indicated, and single-particle "Mie reflectance" (see text), as a function of wavelength.

resulting multiple-scattering function  $F$  for films of three PVCs obtained by the procedure described above is shown in Fig. 3. The function is oscillatory about zero. [Since equation (3) constrains only the convolution of  $F$  with  $G$ , not  $F$  itself, to be positive definite, this is not surprising.]  $F$  is strongly peaked in the backscattering direction, as is expected for a function that embodies the way in which the strongly forward-directed scattering from individual particles is redirected into the backward hemisphere by multiple-scattering events. In a spirit similar to that which led to equation (6), we therefore calculate the "multiple-scattering backscattering fraction"  $F_{\text{back}}$ :

$$F_{\text{back}} = \frac{\int_{-1}^0 |F(\cos \theta)| d(\cos \theta)}{\int_{-1}^1 |F(\cos \theta)| d(\cos \theta)}. \quad (7)$$

The values of  $F_{\text{back}}$  for films of the three PVCs are shown in the inset to Fig. 3. As expected,  $F_{\text{back}} > 0.5$ , meaning that backscattering predominates, and the effect of multiple scattering is to enhance the backscattering over what would occur for a single particle. The single-particle angular distribution function  $G$  for a particle of this size is strongly peaked in the forward direction, with no more than 25% of the scattered light appearing in the backward hemisphere. The high diffuse reflectance observed in TiO<sub>2</sub>-resin films is the result of multiple scattering. As expected, where more particles are present to redirect the incident light into

the backward hemisphere,  $F_{\text{back}}$  increases as the PVC is increased from 1.05% to 1.6%. However, at a PVC of 3%,  $F_{\text{back}}$  is slightly lower than at 1.6%. This can be understood by considering the effects of dependent scattering, i.e., the interaction of the radiation fields of neighboring particles.

In our model of multiple scattering, as in most others, the particles are considered to be independent scatterers. Light that is scattered from one particle is incident upon a second particle, but the presence of the second particle does not alter the radiation field of the first. This is implicit in our use of the single-particle angular distribution function  $G$ . However, numerical calculations in which Maxwell's equations are solved directly in a finite-element model [18–20] have shown that TiO<sub>2</sub> particles begin to interact at surface-to-surface distances  $L$  approximately equal to the wavelength of light in the medium,  $\lambda/n_{\text{medium}}$ . Clusters of particles at this spacing behave similar to a larger single particle, which has more strongly forward-directed scattering. The backscattering fraction is therefore reduced if the particles are brought to within this distance of one another, which for the wavelengths considered here corresponds to 160 nm  $< \lambda/n_{\text{medium}} < 567$  nm. For the smaller PVCs, the average value of  $L$  (assuming the particles are uniformly dispersed) is larger than  $\lambda/n_{\text{medium}}$  for all the wavelengths considered, since  $L = 713$  nm at 1.05% and 593 nm at 1.6%. At these concentrations the particles act as independent scatterers, and  $F_{\text{back}}$  increases with PVC. However, at a PVC of 3% the average value of  $L = 444$  nm, and the radiation fields of adjacent particles influence one another. This reduces the effectiveness of the multiple scattering at redirecting the incident light into the backward hemisphere, and  $F_{\text{back}}$  decreases.

#### 4. CONCLUSIONS

We have analyzed the diffuse reflectance and transmission spectra of TiO<sub>2</sub>-resin films of various concentrations using a multiple-scattering model based on the Kubelka-Munk two-stream formulation [13–15]. We find that for  $\lambda < 400$  nm the spectra are predominantly determined by the scattering properties of the individual single particles. At longer wavelengths, where multiple-scattering effects become important, the particles behave as independent scatterers for volume concentrations of less than approximately 1%. At higher concentrations, where the interparticle spacing becomes less than the wavelength of light in the medium, the interaction of the radiation fields of adjacent particles lowers the backscattering fraction of the multiple-scattering function. This reduction in backscattering is significant for many of the applications of films containing TiO<sub>2</sub>, such as coatings and paper, which rely upon multiple scattering from large numbers of particles to provide the desired opacity.

*Acknowledgements*—The authors would like to thank D. E. Spahr for preparing the samples and for helpful discussions,

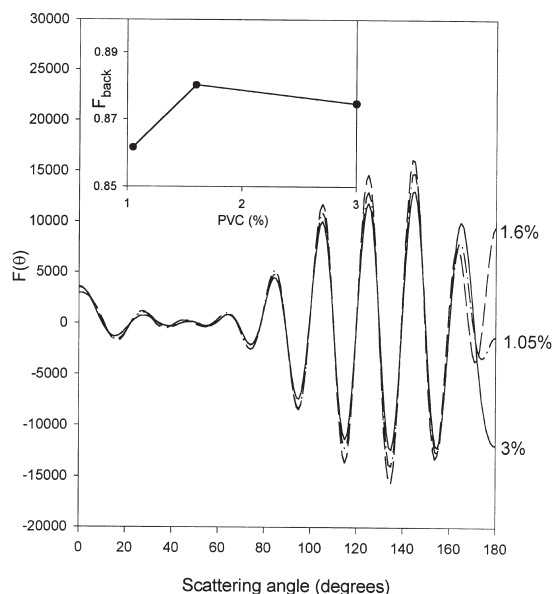


Fig. 3. Multiple-scattering function  $F(\theta)$  (see text) as a function of scattering angle  $\theta$ . Inset: multiple-scattering backscattering fraction  $F_{\text{back}}$  (see text) as a function of particle volume concentration.

and M. F. Lemon for performing the ellipsometry measurements. We are also grateful to A. R. Hanuska and A. Miller for assistance with the Mie scattering calculations.

#### REFERENCES

1. Braun, H., Baidins, A. and Marganski, R. E. *Prog. Organic Coat.*, 1992, **20**, 105.
2. Bohren, C. F. and Huffman, D. R. *Absorption and Scattering of Light by Small Particles*, Wiley & Sons, New York, 1983.
3. van de Hulst, H. C. *Light Scattering by Small Particles*, Wiley & Sons, New York, 1957.
4. Ryde, J. W. *Proc. Roy. Soc. (London)*, 1931, **A131**, 451.
5. Gate, L. F. *J. Phys. D: Appl. Phys.*, 1971, **4**, 1049.
6. Ishimaru, A., Kuga, Y., Cheung, R. L. -T. and Shimizu, K. *J. Opt. Soc. Am.*, 1983, **73**, 131.
7. Maheu, B., Letoulouzan, J. N. and Gouesbet, G. *Appl. Opt.*, 1984, **23**, 3353.
8. Latimer, P. and Noh, S. J. *Appl. Optics*, 1987, **26**, 514.
9. Vargas, W. E. and Niklasson, G. A. *Appl. Optics*, 1997, **36**, 3735.
10. Garg, R., Prud'homme, R. K., Aksay, I. A., Liu, F. and Alfano, R. R. *J. Opt. Soc. Am. A*, 1998, **15**(4), 932.
11. Mudgett, P. S. and Richards, L. W. *Appl. Optics*, 1971, **10**, 1485.
12. McNeil, L. E. and French, R. H., *J. Appl. Phys.*, submitted for publication.
13. Kubelka, P. and Munk, F. *Z. Tech. Physik*, 1931, **12**, 593.
14. Kubelka, P. *J. Opt. Soc. Am.*, 1948, **38**, 448.
15. Kortüm, G. *Reflectance Spectroscopy*, Springer-Verlag, New York, 1969, (J. E. Lohr, Trans.).
16. Saunderson, J. L. *J. Opt. Soc. Am.*, 1942, **32**, 727.
17. Vargas, W. E. and Niklasson, G. A. *Appl. Optics*, 1997, **36**, 5580.
18. Thiele, E. S. and French, R. H. *J. Am. Ceram. Soc.*, 1998, **81**, 469.
19. Thiele, E. S. and French, R. H. *Adv. Mater.*, 1998, **10**, 1271.
20. Thiele, E. S., Ph.D. Thesis, University of Pennsylvania, Department of Materials Science and Engineering, 1998.
21. Ribarsky, M. W. in *Handbook of Optical Constants of Solids*, ed. E. D. Palik, Academic Press, New York, 1985.